Similar patterns of cortical expansion during human development and evolution

Jason Hill[a,1], Terrie Inder[a], Jeffrey Neil[a], Donna Dierker[b], John Harwell[b], and David Van Essen[b]

Departments of [a]Pediatrics and [b]Anatomy and Neurobiology, Washington University School of Medicine, St. Louis, MO 63108

Edited by Pasko Rakic, Yale University, New Haven, CT, and approved June 1, 2010 (received for review February 14, 2010)

The cerebral cortex of the human infant at term is complexly folded in a similar fashion to adult cortex but has only one third the total surface area. By comparing 12 healthy infants born at term with 12 healthy young adults, we demonstrate that postnatal cortical expansion is strikingly nonuniform: regions of lateral temporal, parietal, and frontal cortex expand nearly twice as much as other regions in the insular and medial occipital cortex. This differential postnatal expansion may reflect regional differences in the maturity of dendritic and synaptic architecture at birth and/or in the complexity of dendritic and synaptic architecture in adults. This expression may also be associated with differential sensitivity of cortical circuits to childhood experience and insults. By comparing human and macaque monkey cerebral cortex, we infer that the pattern of human evolutionary expansion is remarkably similar to the pattern of human postnatal expansion. To account for this correspondence, we hypothesize that it is beneficial for regions of recent evolutionary expansion to remain less mature at birth, perhaps to increase the influence of postnatal experience on the development of these regions or to focus prenatal resources on regions most important for early survival.

folding | postnatal | cortex | macaque | primate

The human cerebral cortex is characterized by regional nonuniformities in cellular structure that change with age. Near term, there are regional variations in synaptic density (1, 2), dendritic length, and dendritic spine density (3). Postnatally, synaptic density increases dramatically, reaches a peak density in early childhood, and then undergoes synaptic pruning with a 2-fold or greater reduction (4). The time course of these synaptic changes differs across regions, with primary sensory areas attaining peak density and adult levels earlier than higher order "association" areas (2, 5). In adults, there are large regional nonuniformities in neuronal density (6), dendritic size, branching complexity, and spine density (7).

This evidence for cellular nonuniformities provides grounds for anticipating regional differences in macroscopic aspects of postnatal cortical maturation. Indeed, studies of gray matter volume and overall brain growth provide evidence for complex regional patterns of morphological change during childhood and adolescence (8, 9). We recently used a surface-based approach to compare cortical structure in human term infants to adults. That analysis suggested that although many adult cortical shape characteristics are well established at birth, there may be regional differences in the maturity of cortical folding in term infants compared with adults (10).

Comparisons with nonhuman primates, especially the intensively studied macaque monkey, provide another basis for evaluating regional differences in cortical maturation. Since the evolutionary divergence between humans and macaques ~25 million years ago (11), cortical expansion has been far greater in human lineage than in the macaque lineage. Compared with the macaque cortex, the human cortex has ~10-fold larger surface area and many more cortical areas distinguishable by various methods (12–14). Because this evolutionary expansion in cortical surface area is highly nonuniform (15, 16; translation in ref. 17), a comparison with human postnatal surface expansion may suggest how evolutionary factors have shaped human cortical development.

In the present study, we quantitatively evaluated the maturity of cortical folds at term by comparing cortical shape in a population of term infants and adults and quantifying nonuniformities in human postnatal cortical expansion. By comparing findings in humans and in macaque monkeys, we inferred that the pattern of human evolutionary expansion is impressively similar to the pattern of human postnatal expansion.

Results

Surface Area Expansion During Postnatal Development. We generated cortical surface reconstructions from a population of 12 healthy term-born human infants (10) and compared these reconstructions with corresponding reconstructions from 12 healthy young adults (18). Figure 1 shows a map of cortical surface area expansion between term birth and adulthood. This map was constructed by comparing the average fraction of total surface area occupied by each surface tile in the adult population to its fraction in the term infant population. Although every region of the cortex increases in absolute surface area, the expansion is markedly nonuniform across the cortex. Some regions (orange/yellow) expand as much as 4-fold postnatally (designated as high expansion), whereas others (blue) expand only ~2-fold (designated as low expansion). High-expansion regions are concentrated in lateral temporal, lateral parietal, and dorsal and medial prefrontal regions in both hemispheres. Low-expansion regions are concentrated in medial temporal, occipital, and insular regions. Intermediate expansion (near the average) occurs in posterior temporal, frontopolar, and dorsal parietal regions. To determine which of these patterns are statistically significant, we performed a threshold-free cluster analysis (10, 19) on the fractional surface areas in term infants and adult. Figure 2 shows the locations of significant clusters of high and low expansion overlaid on the cortical expansion maps for the right (Fig. 2*A*) and left (Fig. 2*B*) hemispheres. Black contours enclose regions that expanded significantly more than average (significant high expansion) between infancy and adulthood. White contours enclose regions that expanded significantly less than average (significant low expansion).

Regions passing significance are more extensive in the left hemisphere, but the maps of relative expansion are qualitatively similar in the two hemispheres. To futher address this issue, we

Author contributions: J. Hill, T.I., J.N., and D.V.E. designed research; J. Hill, D.D., and D.V.E. performed research; D.D., J. Harwell, and D.V.E. contributed new reagents/analytic tools; J. Hill, T.I., J.N., D.D., J. Harwell, and D.V.E. analyzed data; and J. Hill wrote the paper.

The authors declare no conflict of interest.

This article is a PNAS Direct Submission.

Freely available online through the PNAS open access option.

Data deposition: All data sets illustrated in this study are accessible in the SumsDB database (http://sumsdb.wustl.edu/sums/directory.do?id=7601585) and can be viewed online (using WebCaret) or offline (using Caret software) as figure-specific "scenes" that recapitulate what is displayed in the individual figure panels.

[1]To whom correspondence should be addressed. E-mail: hillj@wustl.edu.

This article contains supporting information online at www.pnas.org/lookup/suppl/doi:10.1073/pnas.1001229107/-/DCSupplemental.

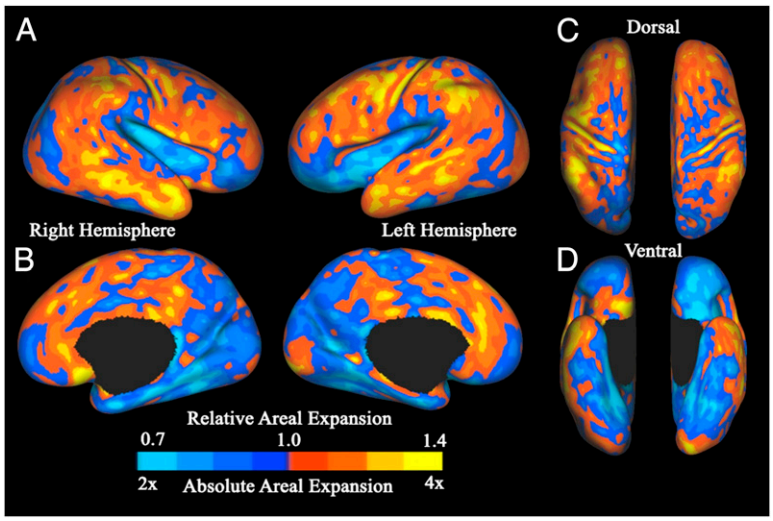

Fig. 1. Postnatal cortical surface expansion. Maps of postnatal cortical surface expansion on the standard mesh average inflated term infant surfaces for both hemispheres, shown in lateral (*A*), medial (*B*), dorsal (*C*), and ventral (*D*) views. The absolute expansion scale indicates how many times larger the surface area of a given region is in adulthood relative to that region's area at term. The relative expansion scale indicates the difference in proportion of total surface area at term birth and adulthood.

performed an interhemispheric correlation analysis that provides greater sensitivity in some regions based on symmetry between the two hemispheres (20). Figure 2*C* shows clusters that expanded significantly more (black outlines) or less (white outlines) than average in both hemispheres. Although the right hemisphere–specific analysis did not reveal significant clusters in the dorsal frontal, lateral parietal, orbitofrontal, or medial frontal regions, portions of these regions are significant when both hemispheres are considered together. Thus, the regional patterns of postnatal cortical surface expansion show a high degree of bilateral symmetry. The residual differences between hemispheres may be related to other developmental asymmetries in brain development (*Discussion*).

The morphological substrates of these relative expansion differences are evident on inspection of individual fiducial surfaces (Fig. 3). Fig. 3 *A–C* shows individual right hemisphere fiducial surfaces for the lateral temporal cortex, a region of significantly high expansion, in three term infants and three adults. The individuals were chosen to span the full range of fractional surface areas within each age group based on the fraction of total cortical surface within a significant cluster of high expansion in the right lateral temporal cortex. For each age group, the top panel (Fig. 3*A*) displays the individual with the smallest fractional surface area; the middle panel (Fig. 3*B*) displays the individual closest to the population mean; and the bottom panel (Fig. 3*C*) displays the individual with the greatest fractional surface area within the significant cluster. Fig. 3 *D–F* displays similar data for the medial temporal and occipital region that undergoes low postnatal expansion.

Qualitatively, in all panels, the lateral temporal cortex (Fig. 3 *A–C*) is distinctly less convoluted in the term infant hemispheres than the adult hemispheres, the convolutions of which are more sharply creased and highly branched. In contrast, the complexity of convolutions in the medial region (Fig. 3 *D–F*) differs little between the term infants and the adults. We quantified this regional difference by computing average sulcal depth for infants and adults in each region. On average, the infant cortex is 47% as deep in the lateral temporal and 67% as deep in the medial occipito-temporal region compared with the corresponding regions

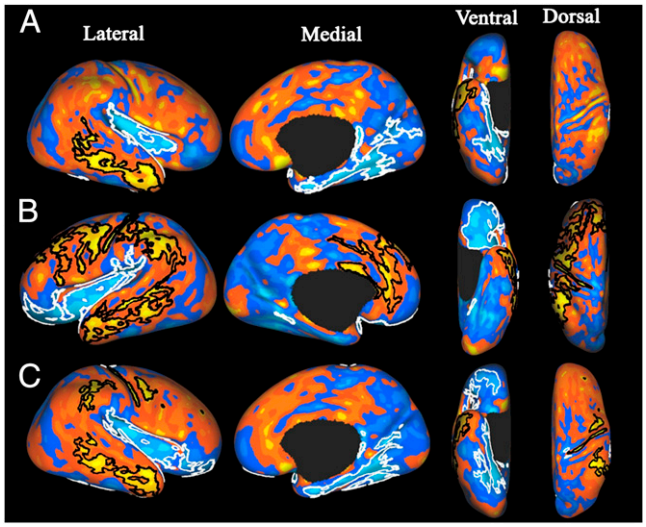

Fig. 2. Statistically significant clusters of nonuniform postnatal cortical surface expansion. Significant clusters for right (*A*) and left (*B*) hemispheres. White contours enclose regions occupying a significantly smaller proportion of the cortex in adulthood than at term. Black contours enclose regions occupying a significantly larger proportion of the cortex in adulthood than at term. (*C*) Statistically significant clusters detected by interhemipsheric symmetry testing.

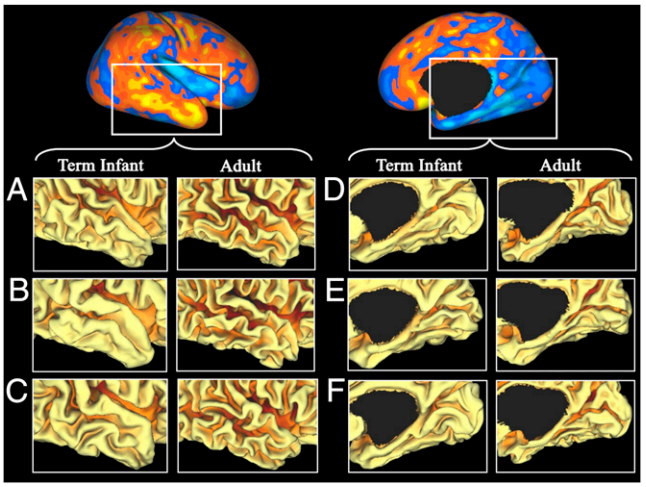

Fig. 3. Individual folding patterns in term infants and adults for regions of high and low postnatal expansion. Individual standard-mesh fiducial surfaces for high-expanding lateral temporal cortex (*A–C*) and low-expanding medial temporal/occipital cortex (*D–F*). White boxes at top show the approximate region being analyzed. For each region, term infant surfaces are shown in the left column of panels, and adult surfaces are shown in the right column of panels.

in adults. Thus, during development a proportionally greater amount of cortex becomes buried in sulci in the higher-expanding regions than in the lower-expanding regions.

Surface Area Expansion During Evolution. Directly studying cortical expansion in human evolution would entail comparisons to evolutionary ancestors using the limited information in the fossil record. Important inferences can nonetheless be made through comparative studies with extant nonhuman primates (13, 21). Human and macaque cortex differ ≈10-fold in total surface area. The ratio of human to macaque cortical surface area is regionally very nonuniform as inferred by interspecies surface-based registration using regions known or strongly suspected to be homologous as registration constraints (15, 22). "Hotspots" with the highest ratios are likely to be regions in which evolutionary expansion was especially rapid in the human lineage. Fig. 4 shows a map of differential cortical expansion for the adult human vs. macaque (Fig. 4*A*) compared with the map of postnatal cortical expansion Fig. 4*B,* left and right hemispheres combined). The pattern of evolutionary expansion is remarkably similar to the map of postnatal cortical expansion. A correlation map between postnatal and evolutionary expansion (Fig. 4*C*) shows a predominance of correlated expansion (red and yellow) rather than anticorrelated expansion (green); regions of near-zero correlation are shown in gray. Dorsal frontal, medial frontal, lateral temporal, and lateral parietal cortices show correlated high postnatal and evolutionary expansion. Medial temporal and occipital regions show correlated low postnatal and evolutionary expansion. Some regions of intermediate evolutionary expansion, including orbito-frontal, insular, and sensorimotor regions, show opposite trends for postnatal and evolutionary expansion.

Discussion

Postnatal Cortical Surface Expansion. We showed previously (10) that human cortical surface area increases 3-fold between term birth and adulthood. By term gestation, almost all neurogenesis and neuronal migration are complete. Accordingly, postnatal surface expansion is presumably dominated by local cellular events, including synaptogenesis, dendritic arborization, gliogenesis, and intracortical myelination. Unexpectedly, the present study shows 2-fold regional nonuniformities in cortical expansion, ranging from 2- to 4-fold expansion across each hemisphere. We hypothesize that cellular and functional nonuniformities at term or in adulthood may contribute to nonuniform cortical expansion. In particular, low-expansion regions may be more structurally and functionally mature at term and/or may have simpler cellular structure in adulthood than high-expansion regions.

Table 1 (rows A–H) summarizes evidence for and against this hypothesis derived from studies (identified by reference numbers) in both humans and macaques. From across the top, selected cortical regions are grouped into low expansion (boldface), intermediate expansion (roman/nonformatted), and high expansion (italic). The rows identify structural and functional factors relevant to our hypothesis, including factors measured near birth (rows A–F) and in adults (rows G and H). Rows I–M list developmental milestones that are reached at different ages within the cortical regions indicated. Numbered entries identify one or more studies examining each factor. Colored boxes denote observations that are consistent (blue) or inconsistent (pink) with our hypothesis. Fig. 5*A* illustrates several consistent and inconsistent regions of interest (ROIs) overlaid on the postnatal expansion map. The relevant characteristics of these ROIs (discussed below) are based on studies in both humans (black lines) and macaque monkeys (colored spheres). We discuss these characteristics in the order presented in Table 1.

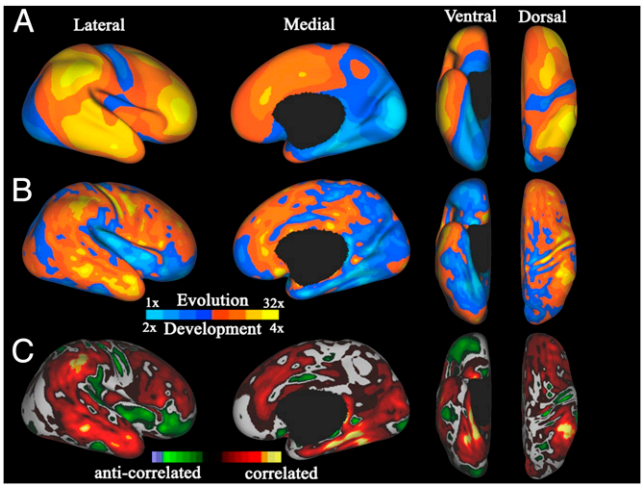

Fig. 4. Comparison of evolutionary and postnatal cortical surface expansion. (*A*) Map of regional evolutionary cortical expansion between an adult macaque and the average human adult PALS-B12 atlas (right hemisphere only). Evolution expansion scale indicates how many times larger the surface area is in humans relative to the corresponding area in the macaque. (*B*) Map of human postnatal cortical expansion (combined left and right hemispheres) for comparison (detailed in Fig. 1 legend). (*C*) Correlation map comparing postnatal to evolutionary cortical surface expansion.

High-Expanding Regions Are Less Mature at Term. At term gestation, regions of high expansion tend to be less mature both structurally and functionally; the opposite tendency holds for low-expanding regions. At a cellular level, this is supported by data on synaptic density. In low-expanding visual and auditory cortex (Heschl's gyrus), synaptic density is 50–100% greater and is closer to peak density than the high-expanding middle frontal gyrus (1). The neonatal macaque visual and auditory cortex are close to mature dendritic spine and dendritic field area, whereas the anterior prefrontal and lateral temporal cortex have approximately half the density and field area found in adulthood (23–25). In newborn humans, the local cerebral metabolic rate for glucose is markedly higher (by 15–25%) in the low-expanding medial temporal and visual cortex than in the high-expanding dorsolateral prefrontal cortex (DLPFC) (26). Accordingly, cortical circuits in the regions of high expansion may be more sensitive to postnatal experience and insult than those in regions of low expansion.

High-Expanding Regions Have Greater Cellular Complexity in Adults. Evidence for regional nonuniformity in cellular complexity of adult cortex comes from quantitative studies of dendritic basal field area, arbor complexity, and spine number. In general, low-expanding regions tend to have smaller and more simply branched dendrites with fewer spines than do high-expanding regions. In humans, dendritic field areas in the high-expanding lateral temporal cortex(Brodmann area 21) are nearly twice the size as in the low-expanding visual cortex (V2) (7). In the adult macaque, dendritic size and complexity vary 3-fold across the cortex: branching patterns are smallest and simplest in low-expanding regions (V1 and V2) (27), intermediate in intermediate-expanding regions (7a, LIPv, and MT) (28–30), and greatest in high-expanding regions (FEF, DLPFC, 7b, STP) (7, 27, 28, 31–34). In adult humans, dendrites have 6-fold more spines and 3-fold greater spine density in the high-expanding lateral temporal (area 21) and frontal (area 10) regions than in the low-expanding visual cortex (V1) (7). Mechanistically, as synapses form and dendritic arbors develop, differential degrees of arbor size and complexity could result in regional differences in the distance between cortical mini-

Table 1. Factors relating to nonuniform postnatal surface expansion

Row	Factor	Visual	Medial temp	Auditory	Dorsal parietal	Post-temp	Fronto-polar	*Lateral tem*	*Lateral parietal*	*Sensori-motor*	*DLPFC*
A	Synaptic density	**1**		**1**							*1*
B	% Peak density	**1**		**1**							*1*
C	Dendritic size	**3**					3			*3*	
D	% Peak spine density	**23**	**23**				23				
E	% Adult dendritic complexity	**24, 25**	**24**	**25**	24			*24*			
F	PET signal	**26**	**26**							*26*	*26*
G	Dendritic complexity	**7, 29**	**29**		28, 29, 30	28, 30	29	*8, 28*	*28*	*34*	*28*
H	Spine number	**8, 23**					8, 23	*8*			
I	Mature synaptic density	**1**		**1**							*1*
J	Mature GM volume	**8**	**8**		8	8		*8*	*8*	*8*	*8*
K	Peak cortical thickness	**36**			36		36	*36*		*36*	*36*
L	Evoked activity		**40, 41**	**39**						*42, 43*	
M	Regional glucose metabolic rate	**38**									*38*

Summary of cellular and functional factors hypothesized to contribute to nonuniform postnatal expansion. Numbered entries identify study or studies examining each factor. Blue and pink boxes denote observations consistent or inconsistent with our hypothesis, respectively. Cortical regions are grouped into low-expansion (boldface), intermediate-expansion (roman/nonformatted), and high-expansion (italic). Row A, synaptic density at term; row B, percentage of peak synaptic density at term; row C, dendritic size (total dendritic length) at term; row D, percentage of peak dendritic spine density at term; row E, percentage of adult dendritic complexity at term; row F, local cerebral metabolic rate for glucose by PET at term; row G, dendritic complexity in adulthood; row H, dendritic spine number in adulthood; row I, temporal sequence of reaching mature synaptic density; row J, temporal sequence of reaching mature gray matter volume; row K, temporal sequence of attaining peak cortical thickness; row L, temporal sequence of detecting evoked cortical activity; row M, temporal sequence of reaching mature distribution pattern of cerebral metabolic rate for glucose. Temp, temporal.

columns (14, 35), with subsequent heterogeneity in the growth of the cortical surface.

High-Expanding Regions Tend to Mature More Slowly. In general, low-expanding regions tend to reach various structural and functional milestones earlier than do high-expanding regions. Mature synaptic density (1), peak cortical thickness (36), and mature values of gray matter density (8, 37) are reached earliest in low-expanding regions (V1 and Heschl's gyrus), later in intermediate-expanding regions (frontopolar and dorsal parietal cortex), and latest in high-expanding regions (DLPFC). Similarly, during the first 3 postnatal mo, PET activity increases more in the low-expanding (V1) than in the high-expanding (DLPFC) regions (26, 38). Activity in the low-expanding auditory cortex in response to sound (39) and medial temporal cortex in response to visually presented faces (40, 41) can be detected by PET imaging or scalp recording within the first 2 postnatal mo. In contrast, transcranial magnetic stimulation of the high-expanding motor cortex does not elicit detectable muscle response in humans until 2 y of age (42, 43).

Subcortical white matter expands dramatically during postnatal maturation, with pronounced regional differences that show some similarities with our data. For example, frontal, anterior temporal, and parietal white matter undergo greater and more protracted maturation than occipital regions, as measured by diffusion imaging and volume expansion (44–47). This could occur if axonal diameters and degree of myelination in underlying white matter are correlated with the maturation of cellular architecture in different

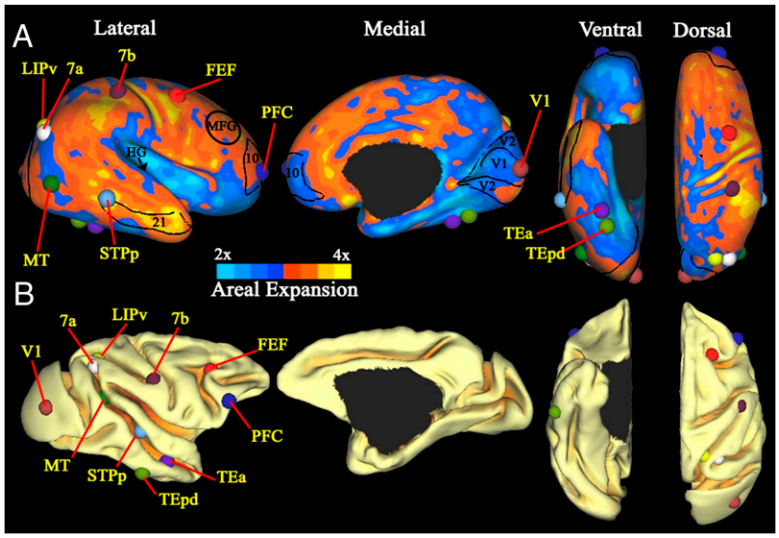

Fig. 5. ROIs mapped to the result of postnatal cortical expansion. (*A*) Postnatal surface expansion map (combined left and right hemispheres) overlaid with ROIs from human and macaque studies. Black outlines identify ROIs from studies in humans. Colored spheres indicate ROIs from studies in macaque monkeys. (*B*) Similar views of the F99 macaque atlas labeled with the macaque ROIs from the top panel indicating the homologous location on the macaque. 10, Brodmann area 10; 21, Brodmann area 21; FEF, frontal eve fields; HG, Heschl's gyrus; LIPv, ventral part of lateral intraparietal cortex; MFG, anterior third of the middle frontal gyrus; MT, medial temporal visual region; PFC, prefrontal cortex; STPp, visual region on anterior bank of superior temporal sulcus; TEa, visual region on the posterior bank of the superior temporal sulcus; TEpd, visual region on the inferior temporal gyrus; V1, primary visual cortex; V2, secondary visual cortex. References for studies used to identify regions of interest: V1, MT, TEa (58); V2, LIP, MT 7a (59); FEF (28); TEpd, PFC (23).

cortical regions: in early-maturing, low-expanding regions, underlying white matter may also mature earlier; in later-maturing, high-expanding regions, underlying white matter may mature later. An alternative hypothesis is that differential expansion of white matter plays a causal role, forcing greater expansion of cortex overlying rapidly growing white matter regions. However, although white matter expansion per se could change the pattern of convolutions, it would not increase cortical surface area except indirectly, through changes in cell size needed to support greater axonal diameters.

Addressing Inconsistencies. The pink boxes in Table 1 indicate apparent inconsistencies between published data and our hypothesis. One notable inconsistency is in sensorimotor cortex. Neonatal cortical neurons in this region are relatively complex (3) and have relatively high local cerebral metabolic rate for glucose (26). They are less complexly branched in adults, albeit with differences among neighboring areas (34). Together these predict lesser postnatal expansion rather than the greater expansion detected. The apparent discrepancies might be reconciled by further studies of cortical microstructure in these regions as well as a finer-grained analysis of cortical expansion. For example, regions with unusually high or low glial or neuronal densities might contribute to high or low expansion, respectively. Species differences might account for inconsistencies in the adult dendritic data, as these are mostly derived from studies in nonhuman primates. Developmental patterns of unique cell types, such as the large Betz cells of the motor cortex (48), may also affect surface expansion. Also, the relatively protracted postnatal development of corticospinal tracts associated with increases in manual dexterity in both macaques (49) and humans (50) may be associated with gray matter changes that contribute to the relatively greater postnatal expansion in the sensorimotor regions.

Cortical thickness is another relevant structural measure. In principle, regions of high expansion might reflect cortex that expanded in surface area preferentially instead of increasing in thickness and vice versa. However, to a first approximation, adult thickness data shows the opposite trend, with high-expanding regions tending to be the thickest and vice versa (51, 52). To address this issue fully, it is critical to know the distribution of cortical thickness at birth; this is further discussed in *SI Text*.

Cortical Expansion During Evolution. Nonuniform cortical expansion during evolution may arise through additional mitotic rounds in specific regions of the proliferative neuronal precursor pool (53), leading to new or enlarged cortical areas. The preset result suggests that many cortical regions that expanded rapidly in evolution were also under evolutionary pressure to remain structurally immature during gestation. In particular, the lateral temporal, parietal, and frontal regions associated with high expansion in human postnatal development and in evolution are generally implicated in higher cognitive functions that distinguish humans from nonhuman primates (21). These regions may have been under pressure to remain immature to do the following: (*i*) to facilitate the contributions of postnatal experience to the development of selected regions; (*ii*) to minimize the use of prenatal resources for development of cortical regions less crucial for early survival; or (*iii*) to limit overall brain size at birth by focusing development/expansion primarily on those areas needed for immediate postnatal survival, thereby minimizing head size as a mechanical obstacle to emergence from the uterus (54). Regions in Fig. 4*C* where there is either no correlation (gray) or an anticorrelation (green) might reflect uncertainty or bias in the comparison between two highly derived measures. Alternatively, they might reflect biologically significant aspects of the complex and poorly understood relationships between cortical evolution and development. Further insights on these issues may emerge from studies of brain circuitry during development that elucidate the nature, timing, and impact of intrinsic and extrinsic developmental signals that control the differentiation and maturation of cortical areas.

Materials and Methods

Subjects and Image Processing. Participant characteristics, MRI scanning, and image processing have been previously described in detail for term infant (10) and adult (18) subjects. Key steps in image processing are illustrated in Fig. S1 and summarized below. Participants consisted of 12 healthy term-born infants (six male and six female\; mean gestational age, 39 wk) from uncomplicated pregnancies and 12 normal right-handed young adults (six male and six female, 18–24 y of age). Institutional review boards approved all procedures and, if appropriate, parents or legal guardians provided informed written consent for the study.

High-resolution T2-weighted and T1-weighted MRI scans were obtained for term infant and adult subjects, respectively. Midcortical segmentation volumes were generated for term infants and adults using the semiautomated LIGASE and SureFit methods, respectively. Cortical surface reconstructions were generated for each hemisphere using tools in Caret (http://brainvis.wustl.edu) (55).

Target Atlas Generation. To quantitatively compare term infant and adult populations without bias toward either age group, a hybrid atlas target was created that reflects the average shape characteristics of both age groups. The hybrid atlas is denoted as the PALS-TA24 atlas because it is a population-average, landmark-and-surface (PALS) atlas derived from a total of 24 term and adult hemispheres. Details concerning atlas construction and registration are given in *SI Materials and Methods*.

Term Infant to Adult Relative Surface Area Expansion. A map of relative cortical surface area expansion between term birth and adulthood was calculated by examining the fractional surface area of each location on the cortex. For each hemisphere of each individual, a map of fractional surface area was calculated by computing the surface area of each fiducial surface tile as the fraction of total cortical surface area (excluding the noncortical medial wall). Maps of relative areal expansion were constructed by dividing the mean fractional area maps of the adults by that of the term infants.

Evolutionary Cortical Surface Expansion. A surface atlas of a single macaque monkey (F99) was previously registered to the adult PALS-B12 atlas using a combination of functional and structural homologies (22). A previously generated map of evolutionary cortical expansion between the macaque monkey and the human adult (15) was registered to the PALS-TA24 atlas. Selected regions of interest were mapped to macaque surface atlas (Fig. 5) according to the following study references: V1, MT, Tea (58); V2, LIP, MT 7a (59); FEF (28); TEpd, PFC (23).

Smoothing. Maps of postnatal surface area expansion and evolutionary area expansion were smoothed 10 iterations (5-mm smoothing kernel) using an average neighbors algorithm (10, 56).

Significance Testing. Regions of significantly high or low postnatal expansion were tested using a two-sample *t* test and an interhemispheric symmetry test.
Two-sample t test. The following operations were performed separately for each hemisphere. (*i*) A two-sample *t* statistic was calculated after spatial smoothing at each surface node from the distribution of term infant and adult fractional surface areas. (*ii*) The group identities (term infant or adult) of each individual fractional area map were randomized 2,500 times, and corresponding *t* maps were generated. (*iii*) To determine statistical significance, a threshold-free cluster enhancement (TFCE) was implemented (10, 19).
Interhemispheric symmetry test. The interhemispheric symmetry analysis tests for significant clusters present in corresponding locations in both hemispheres (20, 57). This method is the same as the two-sample *t* test described above, except that both left and right hemispheres were examined and a *t* correlation map was generated after each permutation by multiplying the two-sample *t* statistic at each surface node in the left hemisphere by the corresponding node in the right hemisphere. This *t* correlation map was used as the *t* statistic for significance testing by threshold-free cluster enhancement.

Data Access and Visualization. All data sets illustrated in this study are accessible in the SumsDB database (http://sumsdb.wustl.edu/sums/directory.do?id=7601585).

ACKNOWLEDGMENTS. We thank Karen Lukas, Jim Alexopolous, Joseph Ackerman, Jr., Jennifer Walker, and Jayne Sicard-Su for subject recruitment, data management, and imaging, respectively; Timothy Coalson for technical assistance; Joshua Shimony, John Pruett, and Brad Schlaggar for valuable discussions and manuscript feedback; and the families and infants who participated in this

study. This project was supported by National Institutes of Health Grants R01HD057098 and R01-MH-60974 (funded by National Institute of Mental Health, *National Institute of Biomedical Imaging and Bioengineering*, National Science Foundation), the Doris Duke Foundation, and the Green Fund. This work was principally funded by the National Institute of Child Health and Development (NICHD HD057098).

1. Huttenlocher PR, Dabholkar AS (1997) Regional differences in synaptogenesis in human cerebral cortex. *J Comp Neurol* 387:167–178.
2. Huttenlocher PR (1990) Morphometric study of human cerebral cortex development. *Neuropsychologia* 28:517–527.
3. Travis K, Ford K, Jacobs B (2005) Regional dendritic variation in neonatal human cortex: A quantitative Golgi study. *Dev Neurosci* 27:277–287.
4. Watson RE, Desesso JM, Hurtt ME, Cappon GD (2006) Postnatal growth and morphological development of the brain: A species comparison. *Birth Defects Res B Dev Reprod Toxicol* 77:471–484.
5. Casey BJ, Tottenham N, Liston C, Durston S (2005) Imaging the developing brain: What have we learned about cognitive development? *Trends Cogn Sci* 9:104–110.
6. Cheung AF, Pollen AA, Tavare A, DeProto J, Molnár Z (2007) Comparative aspects of cortical neurogenesis in vertebrates. *J Anat* 211:164–176.
7. Elston GN, Benavides-Piccione R, DeFelipe J (2001) The pyramidal cell in cognition: A comparative study in human and monkey. *J Neurosci* 21:RC163 1–5.
8. Gogtay N, et al. (2004) Dynamic mapping of human cortical development during childhood through early adulthood. *Proc Natl Acad Sci USA* 101:8174–8179.
9. Sowell ER, et al. (2004) Longitudinal mapping of cortical thickness and brain growth in normal children. *J Neurosci* 24:8223–8231.
10. Hill J, et al. (2010) A surface-based analysis of hemispheric asymmetries and folding of cerebral cortex in term-born human infants. *J Neurosci* 30:2268–2276.
11. Stewart CB, Disotell TR (1998) Primate evolution—in and out of Africa. *Curr Biol* 8: R582–R588.
12. Herculano-Houzel S, Collins CE, Wong P, Kaas JH (2007) Cellular scaling rules for primate brains. *Proc Natl Acad Sci USA* 104:3562–3567.
13. Kaas JH (2008) The evolution of the complex sensory and motor systems of the human brain. *Brain Res Bull* 75:384–390.
14. Mountcastle VB (1997) The columnar organization of the neocortex. *Brain* 120: 701–722.
15. Van Essen DC, Dierker DL (2007) Surface-based and probabilistic atlases of primate cerebral cortex. *Neuron* 56:209–225.
16. Brodmann K (1913) Neue forschungsergebnisse der Grosshirnrindenanatomie mit besonderer berucksichtigung anthropologischer. *Gesselsch Deuts Naturf Artze* 85: 200–240.
17. Elston GN, Garey LJ (2004) *New Research Findings on the Anatomy of the Cerebral Cortex of Special Relevance to Anthropological Questions* (University of Queensland, Brisbane).
18. Van Essen DC (2005) A population-average, landmark- and surface-based (PALS) atlas of human cerebral cortex. *Neuroimage* 28:635–662.
19. Smith SM, Nichols TE (2009) Threshold-free cluster enhancement: Addressing problems of smoothing, threshold dependence and localisation in cluster inference. *Neuroimage* 44:83–98.
20. Van Essen DC, et al. (2006) Symmetry of cortical folding abnormalities in Williams syndrome revealed by surface-based analyses. *J Neurosci* 26:5470–5483.
21. Sherwood CC, Subiaul F, Zawidzki TW (2008) A natural history of the human mind: Tracing evolutionary changes in brain and cognition. *J Anat* 212:426–454.
22. Orban GA, Van Essen D, Vanduffel W (2004) Comparative mapping of higher visual areas in monkeys and humans. *Trends Cogn Sci* 8:315–324.
23. Elston GN, Oga T, Fujita I (2009) Spinogenesis and pruning scales across functional hierarchies. *J Neurosci* 29:3271–3275.
24. Elston GN, Oga T, Okamoto T, Fujita I (2010) Spinogenesis and pruning from early visual onset to adulthood: An intracellular injection study of layer III pyramidal cells in the ventral visual cortical pathway of the macaque monkey. *Cereb Cortex* 20: 1398–1408.
25. Elston GN, Okamoto T, Oga T, Dornan D, Fujita I (2010) Spinogenesis and pruning in the primary auditory cortex of the macaque monkey (Macaca fascicularis): An intracellular injection study of layer III pyramidal cells. *Brain Res* 1316:35–42.
26. Chugani HT, Phelps ME (1986) Maturational changes in cerebral function in infants determined by 18FDG positron emission tomography. *Science* 231:840–843.
27. Elston GN, DeFelipe J (2002) Spine distribution in cortical pyramidal cells: A common organizational principle across species. *Prog Brain Res* 136:109–133.
28. Elston GN, Rosa MG (1998) Complex dendritic fields of pyramidal cells in the frontal eye field of the macaque monkey: Comparison with parietal areas 7a and LIP. *Neuroreport* 9:127–131.
29. Elston GN (2000) Pyramidal cells of the frontal lobe: All the more spinous to think with. *J Neurosci* 20:RC95 1–4.
30. Elston GN, Tweedale R, Rosa MG (1999) Supragranular pyramidal neurones in the medial posterior parietal cortex of the macaque monkey: Morphological heterogeneity in subdivisions of area 7. *Neuroreport* 10:1925–1929.
31. Elston GN (2002) Cortical heterogeneity: Implications for visual processing and polysensory integration. *J Neurocytol* 31:317–335.
32. Elston GN, Elston A, Casagrande V, Kaas JH (2005) Pyramidal neurons of granular prefrontal cortex of the galago: Complexity in evolution of the psychic cell in primates. *Anat Rec A Discov Mol Cell Evol Biol* 285:610–618.
33. Elston GN, et al. (2006) Specializations of the granular prefrontal cortex of primates: Implications for cognitive processing. *Anat Rec A Discov Mol Cell Evol Biol* 288:26–35.
34. Elston GN, Rockland KS (2002) The pyramidal cell of the sensorimotor cortex of the macaque monkey: Phenotypic variation. *Cereb Cortex* 12:1071–1078.
35. Meyer G (1987) Forms and spatial arrangement of neurons in the primary motor cortex of man. *J Comp Neurol* 262:402–428.
36. Shaw P, et al. (2008) Neurodevelopmental trajectories of the human cerebral cortex. *J Neurosci* 28:3586–3594.
37. Toga AW, Thompson PM, Sowell ER (2006) Mapping brain maturation. *Trends Neurosci* 29:148–159.
38. Chugani HT (1998) A critical period of brain development: Studies of cerebral glucose utilization with PET. *Prev Med* 27:184–188.
39. Wakai RT, Lutter WJ, Chen M, Maier MM (2007) On and off magnetic auditory evoked responses in early infancy: A possible marker of brain immaturity. *Clin Neurophysiol* 118:1480–1487.
40. Tzourio-Mazoyer N, et al. (2002) Neural correlates of woman face processing by 2-month-old infants. *Neuroimage* 15:454–461.
41. de Haan M, Nelson CA (1997) Recognition of the mother's face by six-month-old infants: A neurobehavioral study. *Child Dev* 68:187–210.
42. Nezu A, et al. (1997) Magnetic stimulation of motor cortex in children: Maturity of corticospinal pathway and problem of clinical application. *Brain Dev* 19:176–180.
43. Martin JH (2005) The corticospinal system: From development to motor control. *Neuroscientist* 11:161–173.
44. Qiu D, Tan LH, Zhou K, Khong PL (2008) Diffusion tensor imaging of normal white matter maturation from late childhood to young adulthood: Voxel-wise evaluation of mean diffusivity, fractional anisotropy, radial and axial diffusivities, and correlation with reading development. *Neuroimage* 41:223–232.
45. Hua X, et al. (2009) Detecting brain growth patterns in normal children using tensor-based morphometry. *Hum Brain Mapp* 30:209–219.
46. Westlye LT, et al. (2009) Life-span changes of the human brain white matter: Diffusion tensor imaging (DTI) and volumetry. *Cereb Cortex* Dec 23, 2009 [Epub ahead of print].
47. Lebel C, Walker L, Leemans A, Phillips L, Beaulieu C (2008) Microstructural maturation of the human brain from childhood to adulthood. *Neuroimage* 40:1044–1055.
48. Rivara CB, Sherwood CC, Bouras C, Hof PR (2003) Stereologic characterization and spatial distribution patterns of Betz cells in the human primary motor cortex. *Anat Rec A Discov Mol Cell Evol Biol* 270:137–151.
49. Armand J, Edgley SA, Lemon RN, Olivier E (1994) Protracted postnatal development of corticospinal projections from the primary motor cortex to hand motoneurones in the macaque monkey. *Exp Brain Res* 101:178–182.
50. James LM, Halliday DM, Stephens JA, Farmer SF (2008) On the development of human corticospinal oscillations: Age-related changes in EEG-EMG coherence and cumulant. *Eur J Neurosci* 27:3369–3379.
51. Fischl B, Dale AM (2000) Measuring the thickness of the human cerebral cortex from magnetic resonance images. *Proc Natl Acad Sci USA* 97:11050–11055.
52. Hutton C, De Vita E, Ashburner J, Deichmann R, Turner R (2008) Voxel-based cortical thickness measurements in MRI. *Neuroimage* 40:1701–1710.
53. Rakic P (2000) Radial unit hypothesis of neocortical expansion. *Novartis Found Symp* 228:30–42, discussion 42–52.
54. Weiner S, Monge J, Mann A (2008) Bipedalism and parturition: An evolutionary imperative for cesarean delivery? *Clin Perinatol* 35:469–478, ix.
55. Van Essen DC, et al. (2001) An integrated software suite for surface-based analyses of cerebral cortex. *J Am Med Inform Assoc* 8:443–459.
56. Hagler DJ, Jr, Saygin AP, Sereno MI (2006) Smoothing and cluster thresholding for cortical surface-based group analysis of fMRI data. *Neuroimage* 33:1093–1103.
57. Csernansky JG, et al. (2008) Symmetric abnormalities in sulcal patterning in schizophrenia. *Neuroimage* 43:440–446.
58. Elston GN, Tweedale R, Rosa MG (1999) Cortical integration in the visual system of the macaque monkey: Large-scale morphological differences in the pyramidal neurons in the occipital, parietal and temporal lobes. *Proc Biol Sci* 266:1367–1374.
59. Elston GN, Rosa MG (1997) The occipitoparietal pathway of the macaque monkey: Comparison of pyramidal cell morphology in layer III of functionally related cortical visual areas. *Cereb Cortex* 7:432–452.